

The Effect of pH on the Hydrolytic Degradation of Poly(ϵ -caprolactone)-Block-Poly(ethylene glycol) Copolymers

Xian Jun Loh

Department of Chemistry, Melville Laboratory for Polymer Synthesis, University of Cambridge, Cambridge, CB2 1EW, United Kingdom

Correspondence to: X. J. Loh (E-mail: XianJun_Loh@scholars.a-star.edu.sg)

ABSTRACT: The *in-vitro* hydrolytic behavior of diblock copolymer films consisting of poly(ϵ -caprolactone) (PCL) and poly(ethylene glycol) (PEG) was studied at pH 7.4 and pH 9.5 at 37°C. The degradation of these films was characterized at various time intervals by mass loss measurements, GPC, ¹H-NMR, DSC, FTIR, XRD, and SEM. A faster rate of degradation took place at pH 9.5 than at pH 7.4. Analysis of the molecular weight profile during the course of degradation revealed that random chain scission of the ester bonds in PCL predominates at the initial induction phase of polymer degradation. There was also an insignificant mass loss of the films observed. Mass spectroscopy was used to determine the nature of the water soluble products of degradation. At pH 7.4, a variety of oligomers with different numbers of repeating units were present whereas the harsher degradation conditions at pH 9.5 resulted in the formation of dimers. From the results, it can be proposed that a more complete understanding of the degradation behavior of the PCL-*b*-PEG copolymer can be monitored using a combination of physiological and accelerated hydrolytic degradation conditions. © 2012 Wiley Periodicals, Inc. J. Appl. Polym. Sci. 000: 000–000, 2012

KEYWORDS: diblock copolymers; degradation; biodegradable

Received 29 January 2012; accepted 16 March 2012; published online

DOI: 10.1002/app.37712

INTRODUCTION

Biodegradable polymers break down into simpler monomeric or oligomeric components owing to the presence of cleavable chemical bonds present within the polymer backbone. The degradation profile of such a polymer is important in assessing its potential as a biomaterial, particularly in the determination of suitable *in-vivo* applications.¹ For example, the rate of controlled drug release depends primarily on the degradation rate of the encapsulating polymer as the drug is released only upon breakdown of the polymer matrix. Hence the rate of degradation of the chosen polymer must match the desired drug release rate. Furthermore, it is essential to determine the toxicity of the degradation products as well. Much emphasis has been placed on synthesizing and modifying biodegradable polymers such as poly(ϵ -caprolactone) (PCL), poly(lactic acid) (PLA), and poly[(R)-3-hydroxybutyrate] (PHB) because of their potential biomedical applications.^{2–15} In addition to their classical uses as sutures and drug delivery systems, new applications including selectively biodegradable vascular grafts, noninvasive surgical procedures, prevention of postsurgical adhesions and scaffolds in tissue engineering have been created.^{16–23}

PCL is a substantially hydrophobic, semicrystalline aliphatic synthetic polyester which degrades to a naturally occurring metabolite, 6-hydroxyhexanoic acid.¹⁷ The Food and Drug Administration have approved PCL for use in medical and drug delivery devices, making it an excellent candidate for a biomaterial.¹⁸ However, due to its hydrophobic nature, it may not be very useful in certain applications whereby a fast degradation rate is desired. On the other hand, poly(ethylene glycol) (PEG) is a biocompatible and hydrophilic polyether that has been widely used in biomedical research and applications.^{2,5} Through copolymerization, hydrophilic segments of hydrophilic PEG can be incorporated with PCL. This enables the modulation of hydrophilicity and changes the degradation behavior of the copolymer matrix. Recently, there have been many papers which utilize PEG and PCL block copolymers for different biomedical directed applications, such as micelles, nanoparticles, and gels for drug or gene delivery or as tissue engineering scaffolds.^{24–30} It is therefore, increasingly important that there is a thorough degradation study done of this material. Li et al. have studied the hydrolytic degradation of multiblock copolymers comprising PEG and PCL segments under physiological and alkaline

Additional Supporting Information may be found in the online version of this article.

© 2012 Wiley Periodicals, Inc.

conditions.^{31,32} The degradation of PCLs in acidic and basic media have also been studied by Kim et al.³³

A plethora of methods have been used to probe the degradation mechanism of biodegradable polymers as mentioned in the literature. Examples include the examination of the physical mass loss of the films, the molecular weight decrease of the polymers, surface degradation studies, NMR spectroscopic studies, and the isolation and analysis of degradation products.¹¹ The degradation pathway of a polymer occurs in three phases consisting of an incubation period (water uptake), an induction period (molecular weight decrease) and a polymer erosion period (mass loss) as reported by Lee et al.³⁴ For a complete degradation study, these three phases should be monitored together with the examination of both the short-term and long-term degradation behavior of the polymer. Although hydrolytic degradation studies for the PEG-PCL copolymer have been carried out by a few groups, these were neither detailed nor comprehensive enough for the assessment of its suitability as a biomaterial.^{17,18} Therefore, this article attempts to gain a better and more complete understanding of the degradation process of this copolymer by conducting the hydrolysis experiments at different pH values. Degradation at pH 7.4 mimics physiological conditions while accelerated degradation at a higher pH (more hydroxyl ions resulting in faster hydrolysis) would enable the prediction of the long-term behavior. More importantly, the long term degradation would result in the formation of water soluble products. By knowing the composition of the water soluble degradation products, it is hoped that this would enable researchers to predict the toxicity and biocompatibility of these products which are often found at the final stages of degradation.

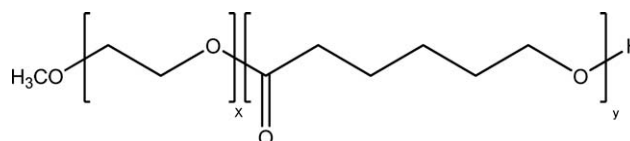
EXPERIMENTAL

Materials and Methods

The copolymer films of PCL-*b*-PEG ($M_n = 20,650$; PEG (M_n) = 2890) used in the experiment were purchased directly from Sigma-Aldrich. The chemical structure of the PCL-*b*-PEG copolymer is given in Scheme 1.

Hydrolysis Experiments

Copolymer films were prepared by solvent casting from a 10 wt % chloroform solution. The resultant films were dried *in vacuo* at 50°C for 2 days, cut into discs (diameter, 8 mm; thickness, 80 μ m) and used for the degradation experiments. After placing the films (≈ 20 mg) into test-tubes, 10 mL of degradation buffer solution at either pH 7.4 or 9.5 was added to the test tubes. The pH 7.4 buffer solution contained 8.0 g of NaCl, 0.2 g of KCl, 1.44 g of Na₂HPO₄, and 0.24 g of K₂H₂PO₄ in 1 L of solution. The pH 9.5 buffer solution contained 3.09 g of H₃BO₃, 3.73 g of KCl, and 1.6 g of NaOH in 1 L of solution. After addition of buffer solution, the test tubes were placed in a water bath maintained at 37°C. Degradation at pH 7.4 was carried out for 20 weeks for the copolymers. For degradation at pH 9.5, the PCL-*b*-PEG copolymers were tested for 20 weeks. Triplicates were prepared for each period of degradation for both pH settings to minimize the effects of random errors. At predetermined time intervals the test tubes were removed from the water bath and the film samples were separated from the buffer solution. These were washed twice with distilled water and sub-



Scheme 1. Structure of PCL-*b*-PEG used in this study.

sequently dried. Lyophilization was carried out for the buffer solution component which contained the water soluble degradation products. Chloroform was added to extract these water soluble products after lyophilization for analysis.

Mass Loss Measurements

The mass loss of the polymer films after degradation was evaluated by eq. (1):

$$\text{Residual mass (\%)} = (M_t/M_0) \times 100\%, \quad (1)$$

where M_t and M_0 were the mass at time t and initial mass, respectively. M_t was obtained after lyophilization of the samples at 50°C for 1 week.

Molecular Characterizations

Molecular weight of the copolymers and their degradation products were determined by gel permeation chromatography (GPC). The ¹H-NMR spectra were recorded on a Bruker AV-400 NMR spectrometer at 400 MHz at room temperature. Fourier transform infra-red (FTIR) spectra of the polymer films coated on a calcium fluoride (CaF₂) plate were recorded on a Bio-Rad 165 FT-IR spectrophotometer; 16 scans were signal-averaged with a resolution of 2 cm⁻¹ at room temperature. Electrospray ionization (ESI) mass spectra were obtained using a Finnigan MAT LCQ spectrometer. The spray voltage was 4.5 kV, and the capillary temperature was set at 250°C.

Differential Scanning Calorimetry Measurements

Differential scanning calorimetry (DSC) measurements were performed on an indium-calibrated TA Instruments 2920 differential scanning calorimeter equipped with an autocoool accessory. The following protocol was used for each sample: Cooling from room temperature to 0°C at 5°C min⁻¹, holding at 0°C for 2 min, heating from 0 to 180°C at 5°C min⁻¹, recooling from 180 to 0°C at 5°C min⁻¹ and finally holding at 0°C for 5 min. Data were collected during the first heating run. Transition temperatures were taken as peak maxima.

Wide-Angle X-Ray Diffraction Measurements

X-ray diffraction (XRD) measurements were carried out by using a Bruker GADDS diffractometer with an area detector operating under Cu K α (1.5418 Å) radiation (40 kV, 40 mA) at room temperature. Film samples were mounted on a sample holder with double-sided adhesive tape.

Field Emission Scanning Electronic Micrograph Imaging

Scanning electronic micrograph (SEM) images were obtained at acceleration voltage of 5 kV on a JSM-6700F microscope (JEOL, Japan). The samples were sputter coated with a thin layer of gold for 15 s to make them conductive before testing.

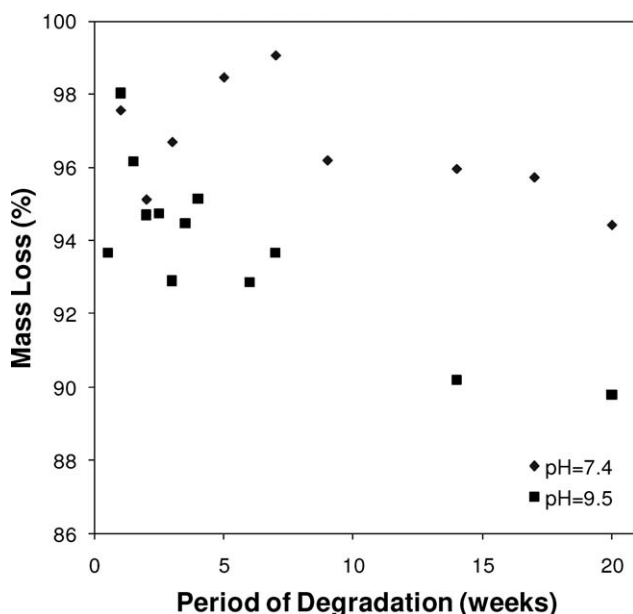


Figure 1. Residual weight (%) of the PCL-*b*-PEG copolymer films after degradation at pH 7.4 and pH 9.5.

RESULTS AND DISCUSSION

Residual Mass Analysis of PCL-*b*-PEG Copolymer Film

The residual mass of the PCL-*b*-PEG copolymer showed an overall decreasing trend over the entire period of degradation at both pHs. The decrease in residual mass could be due to the leaching of cleaved hydrophilic PEG-rich segments into the degradation medium. However, the decrease is very gradual showing a mass loss of only about 6% after 20 weeks of degradation (Figure 1).

The slow decrease in residual mass implied that the bulk copolymer film is hydrolytically stable under physiological conditions for up to 20 weeks. A possible reason for this is that the hydrophilic PEG segment responsible for attracting the hydroxyl groups causing hydrolysis is present in only less than 15 wt % (molecular weight of 2890 out of 20,650) of the total composition. A similar decreasing trend for residual mass was observed for degradation at pH 9.5, with the residual mass at about 90% at the end of Week 20. This was lower than that for degradation at pH 7.4. This suggests that degradation at pH 9.5 could be accelerated compared to that at pH 7.4. Degradation at higher pH is expected to be accelerated because of the presence of a higher concentration of hydroxyl ions (OH^-) which can cleave the ester bonds in the PCL chains. However, the mass loss of about 10% at Week 20 is still rather small, which may be explained by the fact that the copolymer is quite hydrophobic due to the larger proportion of PCL. Previous studies have noted that with the increase of PEG composition, the degradability of the copolymer is enhanced.^{11,17} The other reason is that the degradation of the polymer is still at the induction stage as analyzed in the later section.

Molecular Weight Analysis of PCL-*b*-PEG Copolymer Film

The changes in molecular weight (M_n) of the PCL-*b*-PEG films at various periods of degradation at pH 7.4 and pH 9.5 were determined by GPC. Unimodal GPC profiles of the films were

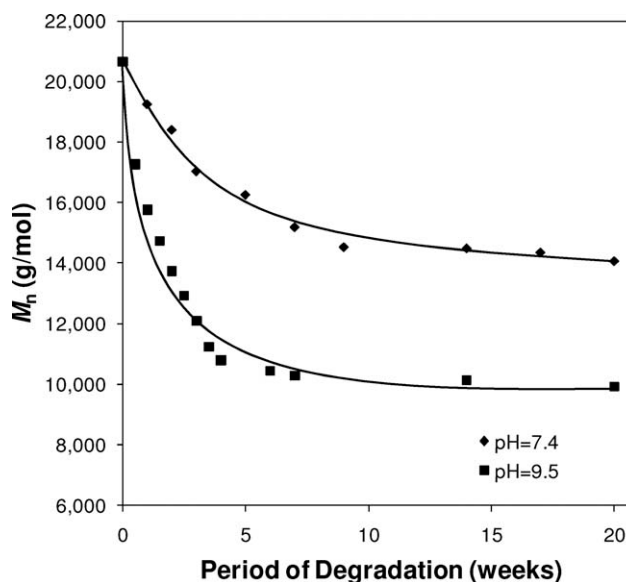


Figure 2. Changes in the molecular weight of the copolymer as a function of time at pH 7.4 and 9.5.

obtained. The molecular weight of PCL-*b*-PEG dropped steadily from Week 1 through to Week 20 (Figure 2). There was a two phase decrease in the molecular weight of the copolymers. For pH 7.4, the decrease in molecular weight was greater for the first 9 weeks as compared with the later weeks of degradation. The results for hydrolysis at pH 9.5 were similar to that at pH 7.4 in that the molecular weights decreased as the period of degradation increased. The decrease in molecular weight was greater for the first 4 weeks as compared with the later weeks of degradation. Figure 2 shows that the decrease in molecular weight was enhanced under a higher pH, particularly in the earlier time intervals.

When the molecular weights of the copolymers are compared at Week 20, the PCL-*b*-PEG copolymer degraded to 9,900 g/mol at pH 9.5. This is much lower than that at pH 7.4 (14,300 g/mol). The basic environment accelerated the cleavage of the ester bonds and also led to a greater number of bonds being cleaved, leading to lower molecular weights in a shorter time.

In addition, the mode of chain scission was determined using the method proposed by Shih.^{35,36} The number of ester bonds in the PCL segment was calculated based on eq. (2):

$$\begin{aligned} \text{Number of ester bond} \\ = \frac{\text{Weight fraction of PCL segment} \times M_n (\text{Polymer chain})}{\text{Molar mass of 1 repeating CL unit}} \quad (2) \end{aligned}$$

The fractional ester bonds (%) were calculated based on eq. (3):

$$E_s = \frac{\text{Number of ester bonds at time } t}{\text{Initial number of ester bonds}} \times 100\% \quad (3)$$

where E_s refers to the fractional ester bonds (%) remaining at time t . Results showed that E_s decreased over the degradation period (Supporting Information Table A11). The rate of

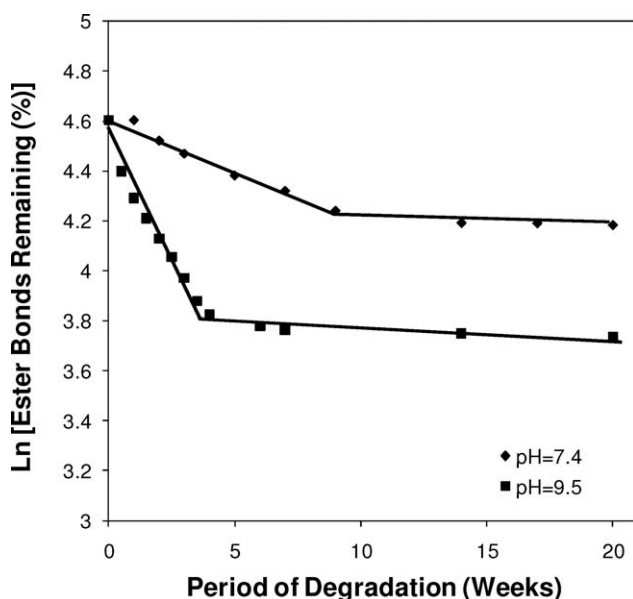


Figure 3. Plot of the natural logarithm of the fractional ester bonds remaining versus degradation time for the degradation occurring at pH 7.4 and 9.5.

decrease of the ester bonds will follow a pseudo-first-order rate kinetics as described by eq. (4):

$$-d[Es]/dt = kEs, \quad (4)$$

where k is the pseudo-first-order-rate constant.

The extent of cleavage of ester bonds was discovered to be dependent on the total number of ester bonds in the polymer chain. At both pHs, there were 2 values for k as seen from the linear natural logarithm plots in Figure 3. At pH 7.4, a higher k value of 0.040 week^{-1} observed in the first 9 weeks meant that

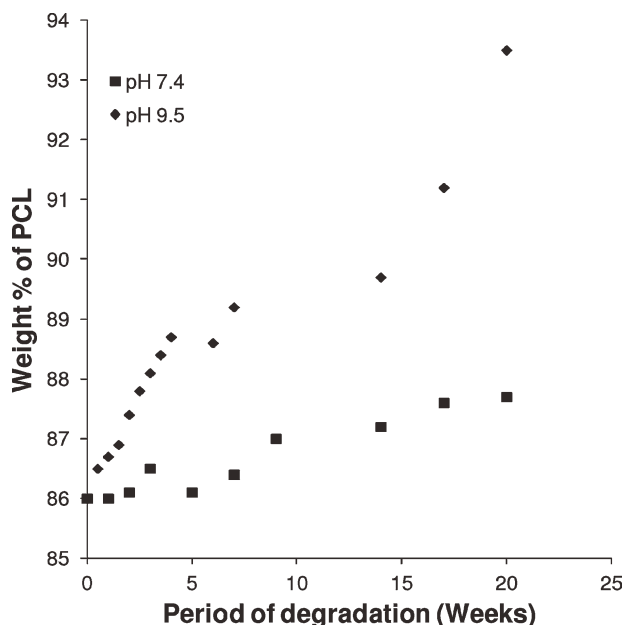


Figure 4. Composition of PCL in the films after degradation at pH 7.4 and 9.5.

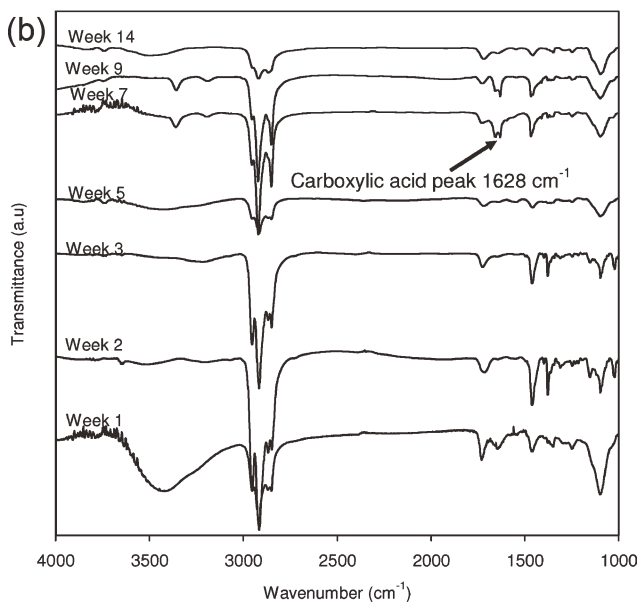
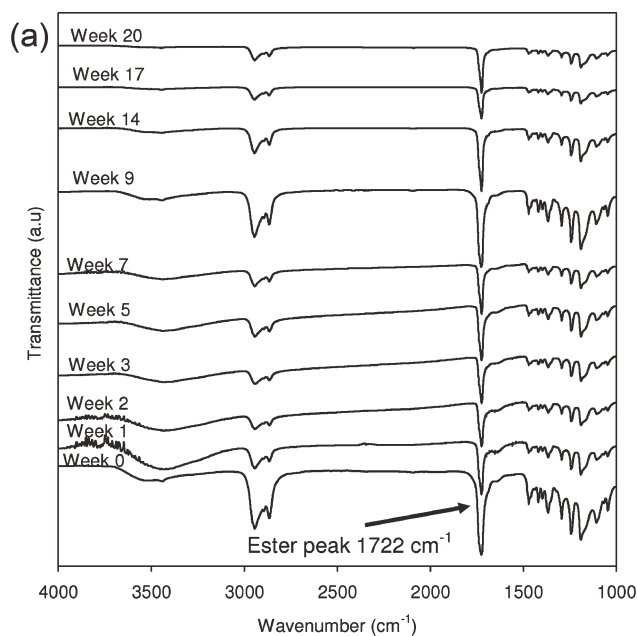


Figure 5. FTIR spectra of degradation products after hydrolysis at pH 7.4 (a) copolymer film and (b) water soluble products.

the rate of cleavage was faster initially because there were more ester bonds remaining, leading to a greater probability of attack by the water molecules. The k value decreased to 0.008 week^{-1} . For pH 9.5, the profiles are similar, except that the transition point takes place after 4 weeks. The initial degradation took place at a rate of 0.212 week^{-1} , this value dropped to 0.0028 week^{-1} beyond 4 weeks.

On the basis of the above analysis, it can be concluded that degradation occurred via random hydrolytic ester cleavage along the PCL segments. Together with the insignificant physical mass loss results in the preceding section, it can be deduced that the copolymer films were at the induction phase of degradation undergoing random chain scission.

Table I. Crystallinity Data for the Copolymer Films After Undergoing Hydrolysis at pH 7.4 as Determined by DSC

Week	PCL					
	T_m (°C)	$\Delta H_o/Jg^{-1}$	wt %	$\Delta H_m/Jg^{-1}$	X_c	PEG wt %
0	64.1	72.41	86.0	84.2	62.2	14.0
1	62.7	81.75	86.0	95.1	70.2	14.0
2	62.9	85.55	86.1	99.4	73.4	13.9
3	63.8	84.62	86.5	97.8	72.3	13.5
5	62.7	87.29	86.1	101.4	74.9	13.9
7	63.0	90.81	86.4	105.1	77.6	13.6
9	63.8	94.47	87.0	108.6	80.2	13.0
14	64.9	97.46	87.2	111.8	82.5	12.8
17	63.6	99.23	87.6	113.3	83.7	12.4
20	64.9	100.8	87.7	114.9	84.9	12.3

Enthalpy change during melting determined in the DSC second heating run. $\Delta H_m) \Delta H_i/W_i$, where ΔH_i is the area of the endothermic peak for the PEG or PCL segment read from the DSC curves and W_i is the weight fraction of the corresponding segment. Crystallinity was calculated from melting enthalpies. Reference values of 205.0 and 139.5 J/g for completely crystallized PEG and PCL were used, respectively.

Compositional Changes of PCL-*b*-PEG Copolymer Film

¹H-NMR analysis was carried out to determine the changes in composition of PEG and PCL segments as the degradation proceeded. A typical ¹H-NMR spectrum for PCL-*b*-PEG copolymer dissolved in CDCl₃ (Week 1 sample) is shown in Supporting Information Figure S1 with the appropriate assignment of peaks corresponding to the respective proton signals from either PEG or PCL. Calculation of the compositions for all films was done by using the integration ratio of resonances at 3.64 ppm for PEG and 4.06 ppm for PCL. The changes in the composition are shown in Figure 4.

The composition of PEG decreased very gradually as hydrolysis advanced while the opposite was true for PCL. PEG composi-

tion fell because the breakage of an ester bond near or at the PEG segment will result in dissolution in the buffer solution since PEG is water soluble. On the other hand, PCL merely lost monomer units of insignificant weight from ester bond cleavage. Thus, the compositional changes in PEG and PCL were expected. However, the difference between the composition of PEG in Week 1 (14.0%) and Week 20 (12.3%) was only 1.7%, suggesting that degradation near the PEG segment was retarded. This outcome, together with the decreasing molecular weight and the insignificant physical mass loss of the copolymer films implies that much of the chains were merely broken up into smaller segments without the formation of water-soluble products leaching into the buffer solution.

Table II. Crystallinity Data for the Copolymer Films after Undergoing Hydrolysis at pH 9.5 as Determined by DSC

Week	PCL					
	T_m (°C)	$\Delta H_o/Jg^{-1}$	wt %	$\Delta H_m/Jg^{-1}$	X_c	PEG wt %
0	64.1	72.41	86.0	84.2	62.2	14.0
0.5	54.1	70.63	86.5	81.7	60.3	13.5
1.0	60.6	84.17	86.7	97.1	71.7	13.3
1.5	61.6	87.23	86.9	100.4	74.1	13.1
2.0	63.3	86.79	87.4	99.3	73.3	12.6
2.5	64.2	87.04	87.8	99.1	73.2	12.2
3.0	62.8	88.20	88.1	100.1	73.9	11.9
3.5	64.0	90.09	88.4	101.9	75.3	11.6
4.0	63.1	91.39	88.7	103.0	76.1	11.3
6.0	65.2	88.54	88.6	99.9	73.8	11.4
7.0	63.4	97.52	89.2	109.3	80.7	10.8
14.0	63.7	99.93	89.7	111.4	82.3	10.3
17.0	64.7	102.60	91.2	112.5	83.1	8.8
20.0	64.8	109.53	93.5	117.1	86.5	6.5

Enthalpy change during melting determined in the DSC second heating run. $\Delta H_m) \Delta H_i/W_i$, where ΔH_i is the area of the endothermic peak for the PEG or PCL segment read from the DSC curves and W_i is the weight fraction of the corresponding segment. Crystallinity was calculated from melting enthalpies. Reference values of 205.0 and 139.5 J/g for completely crystallized PEG and PCL were used, respectively.

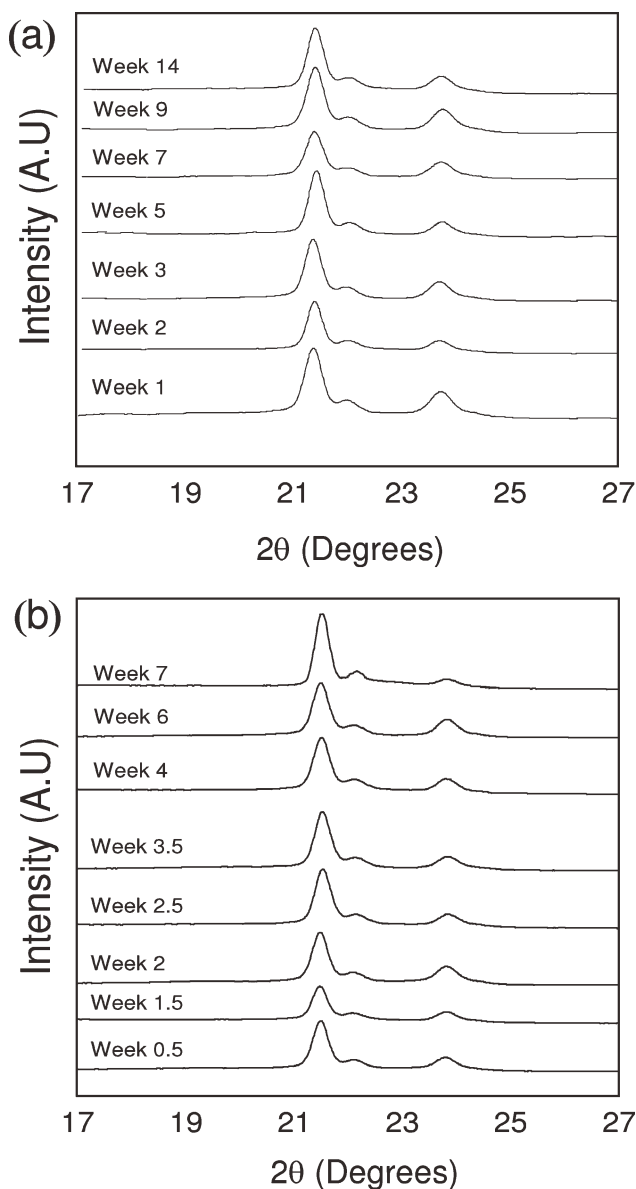


Figure 6. XRD spectra of copolymer films after degradation at (a) pH 7.4 and (b) pH 9.5.

The compositional changes in the PEG and PCL segments after hydrolysis at pH 9.5 can be observed from Table III. PEG composition fell 7.5% between Week 0 (14%) and Week 20 (6.5%). Compared against degradation at pH 7.4 (1.7% in the same time period), accelerated degradation occurring at a higher pH can once again be verified. The greater loss of PEG at this pH suggests that the degradation at pH 9.5 occurs more preferentially near the PEG site. Yet in spite of this, the compositional changes in either the PEG or PCL segment were not accentuated which may again be explained by the hydrophobic nature of the copolymer composition used in this project.

FTIR Analysis of PCL-*b*-PEG Copolymer Film

Fourier transform infra-red spectroscopy was used to probe the functional group changes in the copolymer as the degradation proceeded. The spectra of the samples at various degradation

weeks can be found in Figure 5(a). The original undegraded PCL-*b*-PEG film exhibited a peak at 1722 cm^{-1} , which is due to the stretching of $-\text{COO}-$ of the ester bonds found in PCL.¹¹ Figure 6(b) shows the spectra obtained from the water soluble degradation products. There was no longer a peak at 1722 cm^{-1} , indicating the absence of ester bonds which is due to the hydrophobic nature of PCL. A new peak at 1628 cm^{-1} was observed from 7 weeks onwards and this is attributed to the $-\text{COO}-$ stretch of a carboxylic acid. This carboxylic acid is the product of PCL degradation. The fact that this peak is seen only after 7 weeks indicates that the rate of degradation is slow. Peak values for degradation at pH 9.5 were similar to those observed for pH 7.4 (both film and water soluble products), indicating the presence of ester bonds and carboxylic acid products. The primary difference is the appearance of the carboxylic acid peak at Week 6 as compared with Week 7 for pH 7.4. In all, the two sets of FTIR results confirm that hydrolytic degradation of the PCL-*b*-PEG copolymer occurs through cleavage of the ester bonds in the PCL segment.

Crystallinity Changes in PCL-*b*-PEG Copolymer Film

DSC analysis was used to monitor the changes in crystallinity of the PEG and PCL segments as the degradation period increases. Data were acquired from the first heating run because the intention is to verify the crystalline properties of the film at various time intervals of degradation. The crystallinity of the PCL segment in the copolymer film increased overall. This is because when the PEG segments are removed and its composition fell, it will provide less hindrance to the PCL chains and enable them to arrange themselves suitably, thus attaining higher crystallinity. On the other hand, PEG crystallinity was not detected at all, even at the beginning of degradation and a possible reason is that its original composition was too low relative to the PCL composition and hence its crystallization was totally hampered. The crystallinity data for the various degradation periods can be found in Tables I and II.

XRD Analysis of PCL-*b*-PEG Copolymer Film

XRD analysis was used to support and validate the data obtained from DSC. DSC has its limitations when used to study PCL-*b*-PEG based copolymers because of the proximity of melting temperatures for the PEG and PCL homopolymers (especially when their molecular weights are similar), hence making it difficult to ascribe the melting endotherms to the particular component of this copolymer. XRD is a highly sensitive instrumental method capable of showing the presence of crystalline phases in materials such as polymers more conclusively. Crystalline PCL have peaks at around $2\theta = 21.7^\circ$ and 24.0° while crystalline PEG will have peaks at around $2\theta = 19.4^\circ$ and 23.7° .¹⁷

Figure 6 indicates the presence of crystalline PCL throughout 14 weeks of degradation at pH 7.4 whereas the peak corresponding to crystalline PEG is not observed. The PCL segment has attained higher crystallinity due to its greater composition. On the other hand, as the PCL peak shows, the intensity of the peak increased as the period of degradation progressed. This increase was much faster at pH 9.5 than for pH 7.4. This corroborates well with the results for DSC.

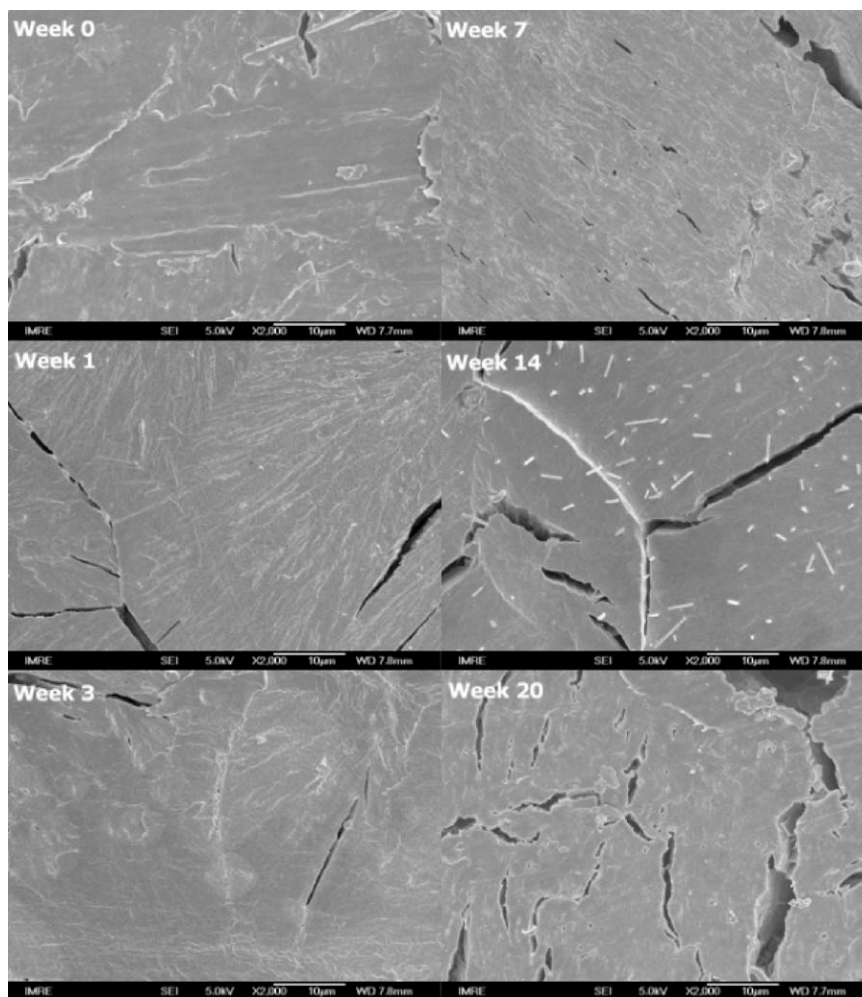


Figure 7. SEM micrographs of block copolymer films at various stages of degradation at pH 7.4

SEM Analysis of PCL-*b*-PEG Copolymer Film

Visual examination of the surface morphology of the degraded copolymer films at various time points was done using SEM. The

micrographs are depicted in Figure 7. Films at Week 1 and 3 of degradation appeared smooth and largely similar to the one at Week 0, implying that degradation has not set in or is largely

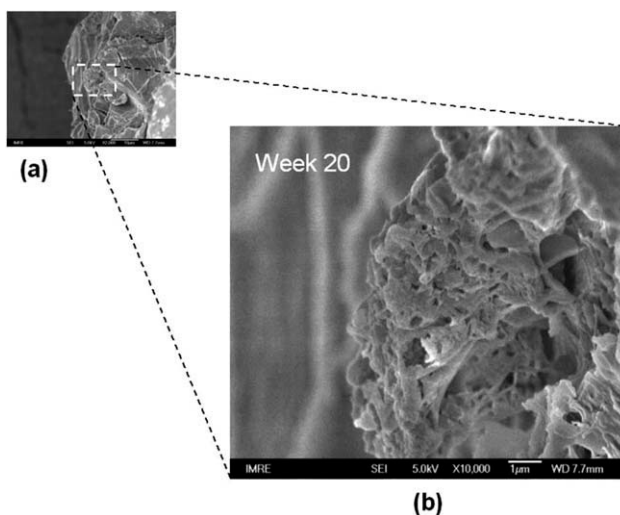


Figure 8. Degradation via edges of copolymer film after 20 weeks of degradation at pH 7.4; (a) at $\times 2000$, (b) at $\times 10,000$.

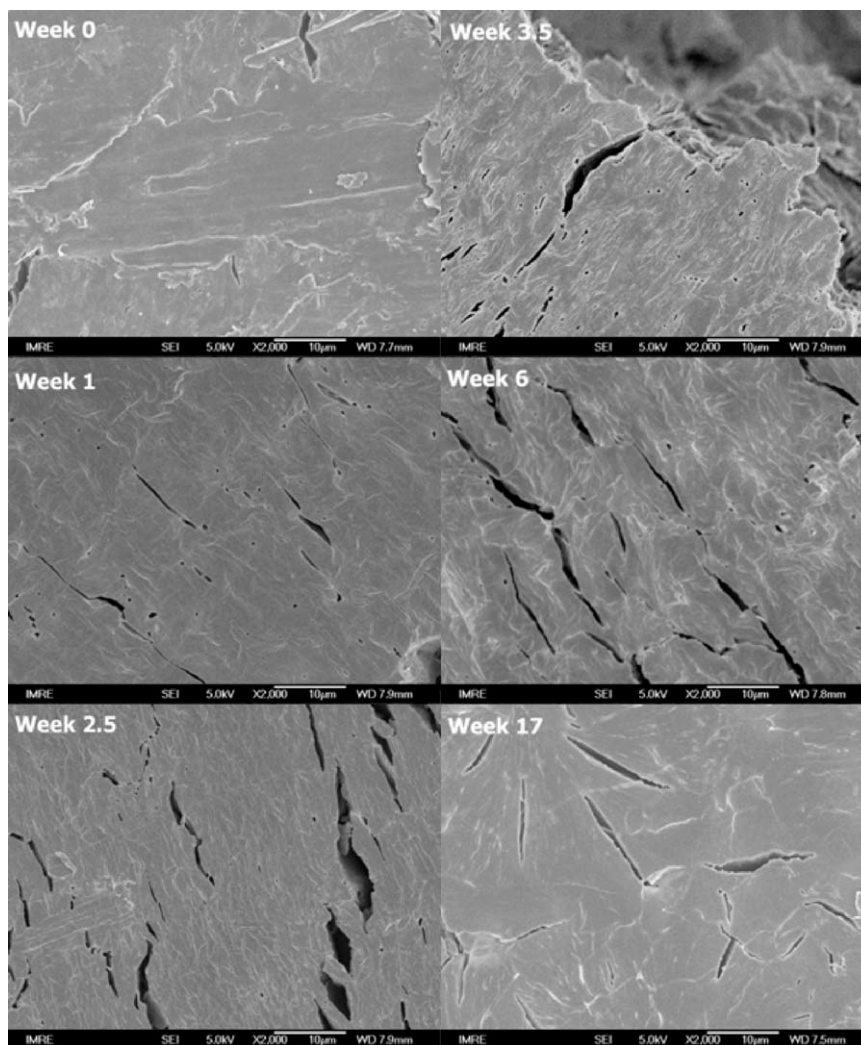


Figure 9. SEM micrographs of block copolymer films at various stages of degradation at pH 9.5.

insignificant. Structural deterioration of the film began only from about Week 7 onwards and some pores (where PEG-rich segments could have broken off and dissolved in the buffer solution) and cracks could be seen. The cracks could be attributed to the increasing crystallinity of the PCL segment (substantiated by DSC results above), causing the films to become more brittle. The intensity and size of the cracks rose as degradation progressed. As shown in Figure 8, a porous network was formed at the edge of the film (Week 20), indicating that degradation most probably transpired via the edges inwards to the rest of the film.

A similar analysis was carried out for the films which were degraded at pH 9.5. Surface deterioration is evident with significant pores and cracks appearing at Week 1 and the porosity and extent of these cracks increased as the hydrolysis period lengthened. This can be observed from Figure 9. The cracks and pores set in much earlier than at pH 7.4, implying that degradation was accelerated to the harsher conditions. The film obtained at the end of Week 20 was also much more brittle than that in previous weeks, proving the enhanced crystallinity of the PCL segments in the copolymer film. Similar to the observation at

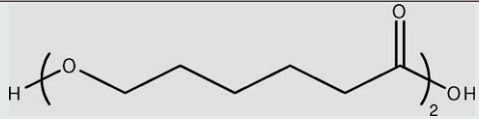
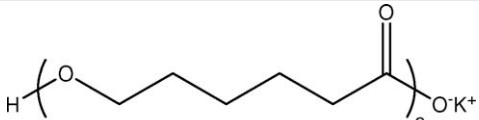
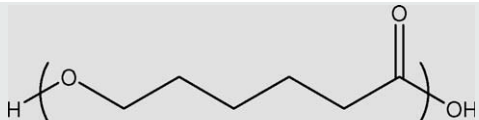
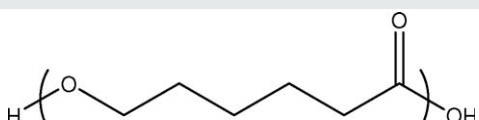
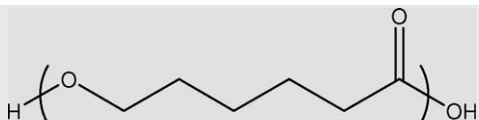
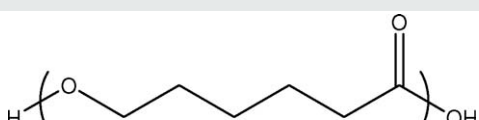
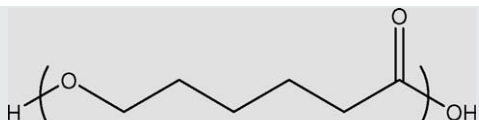
pH 9.5, a porous networked structure was also discovered at the edges of the film under close scrutiny; enforcing the suggestion that degradation occurred via the edges inwards.

Mass Spectroscopy Analysis of Water Soluble Products after Hydrolysis

Mass spectrum of the water soluble products for Week 20 was obtained and the results are shown in Tables III and IV. The mass spectrum is presented in Supporting Information Figures S2 and S3. The PCL segment of the copolymer has been cleaved into a variety of products comprising different number of mer units, including: dimers, dimers coupled with K^+ ion (due to presence of KCl in the buffer solution), trimers, tetramers, pentamers, hexamers, and heptamers. Of these, the majority were the trimers and tetramers.

The dimer coupled with K^+ ion was the main product ascertained in the water soluble products of hydrolysis at higher pH, with a small amount of tetramer. This is in contrast to the results achieved for pH 7.4, and is because the harsher degradation conditions at pH 9.5 has resulted in accelerated cleavage of

Table III. Mass Spectroscopy Results for the Water-Soluble Degradation Products at pH 7.4

Chemical structure	Calculated molecular weight	Observed molecular weight
	246	245.5
	284	283.7
	360	359.5
	474	473.7
	588	587.7
	702	701.5
	816	815.5

the ester bonds to leave only dimers. Other more complex products were present from the mass spectrum but their chemical structures could not be established yet.

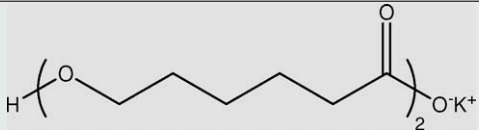
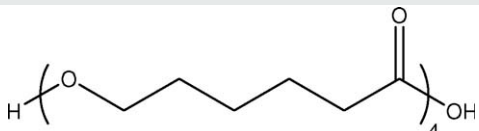
Mechanism for Complete Hydrolytic Degradation of PEG-PCL Copolymers

The SEM micrographs, in conjunction with other data obtained offered a good avenue to propose a degradation mechanism for the copolymer film. From the data of experiments carried out at pH 7.4, the short-term degradation process could be elucidated while accelerated degradation at pH 9.5 allows for the prediction of the long-term hydrolytic degradation behavior of

the copolymers within a shorter time frame. The entire mechanism could be divided into different stages.

Initially, the copolymer entered an induction period whereby very insignificant mass loss was observed. Random chain scission of the ester bond linkages in PCL resulted in a decrease in molecular weight. The SEM micrographs showed that water penetrated through the film edges inwards, similar to the literatures.^{10,15} The polymer erosion stage involved the leaching of the PEG segments and other water soluble oligomeric degradation products into the degradation medium, hence causing a loss in mass. This was validated by the residual mass results,

Table IV. Mass Spectroscopy Results for the Water-Soluble Degradation Products at pH 9.5

Chemical structure	Calculated molecular weight	Observed molecular weight
	284	283.8
	474	473.7

the decreasing PEG weight composition from ^1H NMR analysis and also the data obtained from mass spectroscopy. In particular, mass spectroscopy results revealed that the products formed initially comprised a larger number of mer units before eventually degrading into dimeric products. Furthermore, the dissolution of PEG segments could result in the formation of pores in the film as observed from the SEM micrographs. The products mentioned arose from iterative ester bond scission of the PCL chain. A schematic illustration of the possible degradation process based on the experimental results is shown in Figure 10.

CONCLUSIONS

The *in-vitro* hydrolytic behavior of diblock copolymer films consisting of poly(ϵ -caprolactone) (PCL) and poly(ethylene glycol) (PEG) was studied at pH 7.4 and pH 9.5 at 37°C. By a combination of techniques, the degradation of these films were

characterized at various time intervals by mass loss measurements, molecular weight, compositional and crystallinity changes. A faster rate of degradation took place at pH 9.5 than at pH 7.4. The initial stage of degradation was predominated by random chain scission of the ester bonds in PCL. There was also an insignificant mass loss of the films observed. Mass spectroscopy was used to determine the nature of the water soluble products of degradation. At pH 7.4, a variety of oligomers with different numbers of repeating units were present whereas the harsher degradation conditions at pH 9.5 resulted in the formation of dimers. As these oligomers can be found in the natural metabolites in the body, the degradation fragments are not expected to be toxic to humans. From the results, it can be proposed that a more complete understanding of the degradation behavior of the PCL-*b*-PEG copolymer can be monitored using a combination of physiological and accelerated hydrolytic degradation conditions.

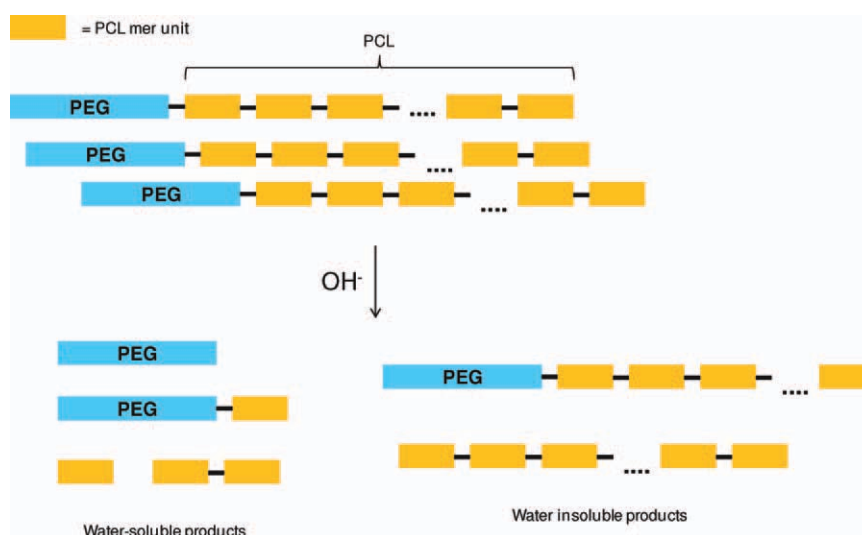


Figure 10. Schematic illustration of degradation process of the copolymer. [Color figure can be viewed in the online issue, which is available at wileyonlinelibrary.com.]

REFERENCES

1. Hutmacher, D. W. *J. Biomater. Sci.: Polym. Ed.* **2001**, *12*, 107.
2. Li, X.; Loh, X. J.; Wang, K.; He, C. B.; Li, J. *Biomacromolecules* **2005**, *6*, 2740.
3. Loh, X. J.; Cheong, W. C. D.; Li, J.; Ito, Y. *Soft Matter* **2009**, *5*, 2937.
4. Loh, X. J.; Goh, S. H.; Li, J. *Biomaterials* **2007**, *28*, 4113.
5. Loh, X. J.; Goh, S. H.; Li, J. *Biomacromolecules* **2007**, *8*, 585.
6. Loh, X. J.; Goh, S. H.; Li, J. *Phys. Chem. B* **2009**, *113*, 11822.
7. Loh, X. J.; Gong, J. S.; Sakuragi, M.; Kitajima, T.; Liu, M. Z.; Li, J.; Ito, Y. *Macromol. Biosci.* **2009**, *9*, 1069.
8. Loh, X. J.; Li, J. *Expert Opin. Ther. Pat.* **2007**, *17*, 965.
9. Loh, X. J.; Peh, P.; Liao, S.; Sng, C.; Li, J. *J. Controlled Release* **2010**, *143*, 175.
10. Loh, X. J.; Sng, K. B. C.; Li, J. *Biomaterials* **2008**, *29*, 3185.
11. Loh, X. J.; Tan, K. K.; Li, X.; Li, J. *Biomaterials* **2006**, *27*, 1841.
12. Loh, X. J.; Tan, Y. X.; Li, Z. Y.; Teo, L. S.; Goh, S. H.; Li, J. *Biomaterials* **2008**, *29*, 2164.
13. Loh, X. J.; Wang, X.; Li, H. Z.; Li, X.; Li, J. *Mater. Sci. Eng. C-Biomimetic Supramol. Syst.* **2007**, *27*, 267.
14. Loh, X. J.; Wu, Y. L.; Seow, W. T. J.; Norimzan, M. N. I.; Zhang, Z. X.; Xu, F.; Kang, E. T.; Neoh, K. G.; Li, J. *Polymer* **2008**, *49*, 5084.
15. Loh, X. J.; Zhang, Z. X.; Wu, Y. L.; Lee, T. S.; Li, J. *Macromolecules* **2009**, *42*, 194.
16. Cohn, D.; Elchai, Z.; Gershon, B.; Karck, M.; Lazarovici, G.; Sela, J.; Chandra, M.; Marom, G.; Uretzky, G. *J. Biomed. Mater. Res.* **1992**, *26*, 1185.
17. Cohn, D.; Stern, T.; Gonzalez, M. F.; Epstein, J. *J. Biomed. Mater. Res.* **2002**, *59*, 273.
18. Huang, M. H.; Li, S. M.; Hutmacher, D. W.; Schantz, J. T.; Vacanti, C. A.; Braud, C.; Vert, M. *J. Biomed. Mater. Res. A* **2004**, *69*, 417.
19. Jeong, B.; Bae, Y. H.; Kim, S. W. *J. Biomed. Mater. Res.* **2000**, *50*, 171.
20. Jeong, B.; Bae, Y. H.; Lee, D. S.; Kim, S. W. *Nature* **1997**, *388*, 860.
21. Peter, S. J.; Miller, M. J.; Yasko, A. W.; Yaszemski, M. J.; Mikos, A. G. *J. Biomed. Mater. Res.* **1998**, *43*, 422.
22. Sawhney, A. S.; Pathak, C. P.; Vanrensburg, J. J.; Dunn, R. C.; Hubbell, J. A. *J. Biomed. Mater. Res.* **1994**, *28*, 831.
23. Storck, M.; Orend, K. H.; Schmitzrixen, T. *Vasc. Surg.* **1993**, *27*, 413.
24. Chan-Park, M. B.; Zhu, A. P.; Shen, J. Y.; Fan, A. L. *Macromol. Biosci.* **2004**, *4*, 665.
25. Hua, C.; Dong, C. M. *J. Biomed. Mater. Res. A* **2007**, *82*, 689 2007.
26. Kim, M. S.; Seo, K. S.; Khang, G.; Cho, S. H.; Lee, H. B. *J. Polym. Sci. A: Polym. Chem.* **2004**, *42*, 5784.
27. Kim, T. G.; Lee, D. S.; Park, T. G. *Int. J. Pharm.* **2007**, *338*, 276.
28. Ma, Z. S.; Haddadi, A.; Molavi, O.; Lavasanifar, A.; Lai, R.; Samuel, J. *J. Biomed. Mater. Res. Part A* **2008**, *86*, 300.
29. Shenoy, D. B.; Amiji, M. A. *Int. J. Pharm.* **2005**, *293*, 261.
30. Xiong, X. B.; Uludag, H.; Lavasanifar, A. *Biomaterials* **2009**, *30*, 242.
31. Li, S. M.; Chen, X. H.; Gross, R. A.; McCarthy, S. P. *J. Mater. Sci.: Mater. Med.* **2000**, *11*, 227.
32. Li, S. M.; Garreau, H.; Vert, M.; Petrova, T.; Manolova, N.; Rashkov, I. *J. Appl. Polym. Sci.* **1998**, *68*, 989.
33. Jung, J. H.; Ree, M.; Kim, H. *Catal. Today* **2006**, *115*, 283.
34. Lee, J. W.; Gardella, J. A. *Macromolecules* **2001**, *34*, 3928.
35. Shih, C. *Pharm. Res.* **1995**, *12*, 2036.
36. Shih, C. *J. Controlled Release* **1995**, *34*, 9.